processes

MDPI

Article

Effect of Vertical Permeability Heterogeneity in Stratified Formation on Electricity Generation Performance of Enhanced Geothermal System

Yuchao Zeng [1], Fangdi Sun [2,*] and Haizhen Zhai [3]

[1] National-Regional Joint Engineering Research Center for Soil Pollution Control and Remediation in South China, Guangdong Key Laboratory of Integrated Agro-Environmental Pollution Control and Management, Institute of Eco-Environmental and Soil Science, Guangdong Academy of Sciences, Guangzhou 510650, China; zengyuc@126.com
[2] School of Geography and Remote Sensing, Guangzhou University, Guangzhou 510006, China
[3] Guangzhou Institute of Energy Conversion, Chinese Academy of Sciences, Guangzhou 510640, China; zhaihz@ms.giec.ac.cn
* Correspondence: sfd_geo@gzhu.edu.cn

Abstract: Because geologic sedimentation and hydrofracturing processes are not homogeneous, the reservoirs of enhanced geothermal systems (EGSs) are also heterogeneous; this has a significant influence on the electricity generation performance of EGS. Presently, there are a lack of systematic and profound studies on the effect of vertical permeability heterogeneity in stratified formation on the electricity generation performance of EGS. In order to uncover the effect of vertical permeability heterogeneity on electricity generation performance of EGS, in this work we analyzed the influence of vertical permeability heterogeneity on electricity generation performance of EGS through a numerical method based on geological data at the Yangbajing geothermal field. The results indicate that when the average permeability of stratified formations is constant for a homogeneous reservoir, the system attains maximum water production rate, maximum electric power, minimum reservoir impedance and maximum pump power; with the increasing of the vertical permeability heterogeneity, the water production rate gradually decreases, the electric power gradually declines, the reservoir impedance gradually increases and the pump power gradually declines. When the average permeability of stratified formations is constant, with the increasing of the vertical permeability heterogeneity, the injection pressure and energy efficiency only changes very slightly; this indicates that the vertical permeability heterogeneity is not the main factor affecting the system injection pressure and energy efficiency.

Keywords: vertical permeability heterogeneity; reservoir permeability; enhanced geothermal system; electricity generation performance; Yangbajing geothermal field

Citation: Zeng, Y.; Sun, F.; Zhai, H. Effect of Vertical Permeability Heterogeneity in Stratified Formation on Electricity Generation Performance of Enhanced Geothermal System. *Processes* **2021**, *9*, 744. https://doi.org/10.3390/pr9050744

Academic Editor: Song Hu

Received: 2 April 2021
Accepted: 20 April 2021
Published: 22 April 2021

1. Introduction

1.1. Background

The EGS geothermal resource is the main body of the whole geothermal resource. The total EGS resource within a 10 km depth that can be exploited occupies more than 90% of the geothermal resource [1], so only the development and utilization of the EGS resource opens the inventory of the geothermal resource. Compared with other renewable energy sources, the EGS resource is more concentrated and stable and very suitable for generating base-load electric power, with a high utilization efficiency and nearly no pollution emission [1,2]. Therefore, the development of EGS resources has received worldwide attention. The total EGS resource reserve in China within a 3–10 km depth amounts to 20.90 M EJ; if the recoverable fraction is taken as 2%, the recoverable EGS resource amounts to 4400 times the total annual energy consumption in 2010 in China [3]. It is predicted that humans will utilize EGS on a large scale to generate electricity by 2030, and EGS will provide

about 100,000 MW electric power by 2050 in the U.S.A., occupying about 10% of the total electricity generating capacity [1].

Because numerical studies of EGS reservoir are timesaving, inexpensive and relatively easy, numerical simulations are of great significance for analyzing the characteristics of the long-term electricity generation performance of EGS [1,2]. Zeng et al. investigated the performance and efficiency characteristics of EGSs through vertical wells and horizontal wells at the Desert Peak geothermal field, and found that reservoir impedance through a single vertical fracture is within 1.14–1.93 MPa/(kg/s), which is far higher than the commercial criterion of 0.1 MPa/(kg/s); the reservoir impedance through two horizontal wells is within 0.10–0.13 MPa/(kg/s), which is very close to the commercial criterion, so adopting two horizontal wells can obtain better heat production and electricity generation performance [4,5]. Based on the geological data at Yangbajing geothermal field, Zeng et al. numerically studied the electricity generation performance of EGSs through a single horizontal well, a single vertical well, multi vertical wells and multi horizontal wells, respectively, and found that the heat recovery ratio of a single well system is very low and adopting multi wells can obtain a higher heat recovery ratio [2,6–9]. Zhang et al. researched the electricity generation performance and efficiency characteristics of EGS through two horizontal wells at the Xujiaweizi area at the Daqing oilfield, and found that during the past 20 years, the reservoir impedance has been within 0.17–1.49 MPa/(kg/s), which is far higher than the commercial criterion of 0.1 MPa/(kg/s), so the horizontal well technology still needs to be improved [10]. Zhang et al. numerically investigated the electricity generation and heating potential of the enhanced geothermal system in Songliao Basin, and the results indicate that Yingcheng formation is suitable for the development of HDR (hot dry rock) resources in this region [11]. Zhang et al. numerically evaluated the potential of developing an enhanced geothermal heating system in northeast China, and the results demonstrate that thermal energy production from the stimulated reservoir is satisfactory for heating purposes, but the water flow impedance maintains at a relatively high level during the production period [12]. Huang et al. forecasted the heat extraction and electricity production of a prospective enhanced geothermal system site in Songliao Basin, and the results suggest that the desirable thermal efficiency and gross power output could be obtained initially, whereas the decrease in production arising from thermal depletion of the reservoir is significant at later stages of the operation [13]. Huang et al. conducted a parametric study of an enhanced geothermal system based on thermo–hydro–mechanical modeling of a prospective site in Songliao Basin, and the results show that the properties that are able to strengthen the heat convection in the reservoir are able to influence the power output significantly, and a wellbore arrangement that takes advantages of the buoyancy flow is also a valuable way to increase the production [14].

Besides simulations in the geothermal field scale as stated above, the theory for simulating fractured EGS reservoirs have made great progress in recent years [15–18]. First, besides the equivalent porous media (EPM) method to represent the fractured reservoirs, the double porosity method (DPM) [19–23], the multiple interacting continua (MINC) method [24–26] and the discrete fracture network (DFN) method [27–32] are increasingly used. Sanyal et al. used the DPM method to investigate the productivity of typical EGS, and found that fracture spacing has a significant influence on the electric power [19]. Taron et al. established a thermal–hydrologic–mechanical–chemical model based on the DPM method, and this greatly improved the simulation accuracy for EGS reservoirs [20,21]. Gelet et al. employed the DPM method to study the heat production performance of EGS and found that the single porosity approach overestimates the thermal contraction of fractured reservoirs [22,23]. Pruess et al. used the MINC method to study the production behavior of enhanced geothermal systems with CO_2 as the working fluid, and the results showed strong effects of gravity on the mass flow and heat extraction due to the large contrast of CO_2 density between cold injection and hot production conditions [24,25]. Zeng et al. investigated the electricity generation potential at the Yangbajing geothermal field through the MINC method, and found that the system attained an electric power of 22.2–19.3 MW and an energy efficiency

of 23.92–10.82 during 30 years through five vertical wells [26]. Because the DFN method can accurately reflect the heterogeneity and anisotropy of the fractured reservoirs, it has become a hot spot for EGS reservoir modeling, such as the studies reported in [27–32]. Second, traditional EGS modeling mainly considers the coupling hydrological–thermal effect, while in recent years, the three coupling effects of the hydrological–thermal–mechanical model or four coupling effects of the hydrological–thermal–mechanical–chemical model are considered more and more in simulations [15–18,27–31]. Pandey et al. summarized the latest advances in the hydrological–thermal–mechanical–chemical model for EGS, and found that the poroelastic effects are important for short time periods (hours to days), the thermoelastic effects are important for intermediate time periods (days to months) and the chemical effects are important for long time period (months to years) [18]. Salimzadeh et al. presented a coupled hydraulic–thermal–mechanical–chemical model for EGS reservoirs and studied the aperture change under in situ stresses during heat production [27]. Shi et al. investigated heat extraction performance of a multilateral-well EGS based on a hydraulic–thermal–mechanical model and found that reservoir properties have significant effects on rock deformation [28]. Wang et al. proposed a strongly coupled hydro-thermo–mechanical model to simulate the heat production process in Habanero EGS and the results demonstrate that the proposed model is robust and effective [29]. Sun et al. studied heat extraction in EGS with the hydraulic–thermal–mechanical model based on the discrete fracture model, and the results indicate that it is important to take into account the HTM coupling effects [30]. Yao et al. used a hydraulic–thermal–mechanical model to simulate the Desert Peak geothermal reservoir and the results show that the electric power can meet the commercial standard [31]. Third, different from the traditional thermal model which assumes that water and rock are in local thermodynamic equilibrium, recently, the local thermodynamic non-equilibrium model isapplied more and more [33–35]. Jiang considered the actual existence of a local thermal non-equilibrium between the rock matrix and flowing fluid in the porous heat reservoir, and established a three-dimensional transient model for the EGS subsurface thermo-hydraulic process [33,34]. Shaik et al. simulated fluid–rock coupling heat transfer in a naturally fractured geothermal system that considered the local thermal non-equilibrium effect, and the results show that the heat transfer between rock and fluid and the fracture connectivity have a profound effect on the economic potential of a geothermal reservoir [35].

Presently, in most EGS reservoir models, the reservoir is assumed as homogeneous, and the effect of the permeability heterogeneity of the layered reservoirs on the heat production and electricity generation is neglected [1]. In fact, because the geologic sedimentation and hydrofracturing processes are not homogeneous and the EGS reservoirs are also layered and heterogeneous, the influence of the heterogeneity of reservoirs on production performance should be taken into consideration in simulation studies [1]. In order to study the effect of the vertical permeability heterogeneity of the EGS reservoirs on the heat production and electricity generation performance, in this work, we investigated the influence of the permeability heterogeneity on the production performance through a numerical simulation based on the geological data at the Yangbajing geothermal field. The geologic structure, and hydrological and geothermal features of the Yangbajing geothermal field are reported in references [6,36,37], in detail. This will lay a solid foundation for future research and the development of EGS [1].

1.2. Research Objectives

The research objectives of this work are to investigate the effect of the vertical permeability heterogeneity of the EGS reservoirs on heat production and electricity generation performance, and to find out the optimum reservoir permeability conditions for the electricity generation of EGS reservoirs. This will provide guidance for the future site selection and performance optimization of EGS.

2. Numerical Method

2.1. Physical–Mathematical Model

According to experiences of numerical simulation studies of heat mining, in this work, we used the five-spot well configuration, as shown in Figure 1 [8]; one injection well is located in the center and four production wells are located at the corners. The distance between two adjacent production wells is 1000 m. Because of symmetry, only one fourth of the model domain needs to be simulated, as the grey fraction shown in Figure 1. Based on the geological data at the Yangbajing geothermal field, the deep fractured granite reservoir is located within 950–1350 m, and thickness of the reservoir is 400 m. Assuming, after stimulation, the average fracture spacing is lower than 2–3 m, the heat transfer between the cap rock or base rock and the reservoir can be neglected [6]. Because the average fracture spacing is lower than 2–3 m, the local thermodynamic equilibrium between the fractured rock and circulating water is reasonable [4], thus the fractured granite reservoir can be represented as an equivalent porous medium [2,4–9]. The cold water enters into the reservoir through the perforated interval of 50 m length at the bottom position of the injection well and leaves the reservoir through the perforated interval of 50 m length at the top position of the production well. This kind of production scheme can greatly prolong the reservoir lifetime, reduce the reservoir impedance and improve the production efficiency [2]. In this study, we used the TOUGH2-EOS1 codes to carry out the simulations, which was developed at the Lawrence Berkeley National Laboratory [38]. The TOUGH2 codes employed the integral finite difference method to solve the conservation equations of mass, momentum and energy, and the comparison between the computation through TOUGH2 codes and the experiment has proved that the calculation results are highly reliable [38]. The governing equations of fluid flow and heat transfer based on the equivalent porous medium method can be found in [38].

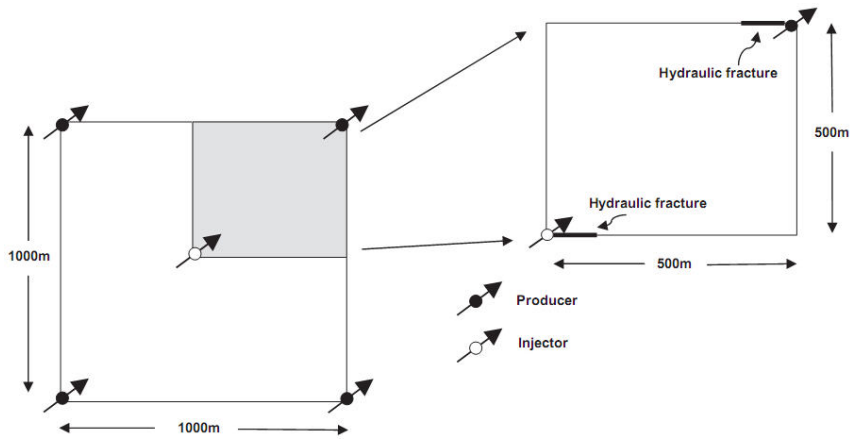

Figure 1. Well configuration of the 950–1350 m fractured granite reservoir.

In order to investigate the influence of vertical permeability heterogeneity in stratified formation on the system heat production, we equally divided the 950–1350 m reservoir into 8 layers with different permeabilities; the thickness of every layer is 50 m and the horizontal and vertical permeability in each layer are different. In this study, we neglected the dependence of permeability on the reservoir porosity and assumed that all porosities in each layer are 0.10 [39]. The average horizontal permeability of the 8 layers was kept equal at 50×10^{-15} m^2. We assumed that the ratio of the horizontal permeability k_h to the vertical permeability k_v is constant as $k_h/k_v = \alpha$ [39]. The degree of reservoir vertical heterogeneity is given by the non-dimensional parameter β as Equation (1) deduced by Luo et al., where N is the total numbers of layers, $k_{h,i}$ and $h_{v,i}$ are the horizontal and vertical permeability of the ith layer, $k_{h,m}$ is the mathematical average of all the horizontal permeability and $k_{v,m}$ is the mathematical average of all the vertical permeability. The definition of $k_{h,m}$ and $k_{v,m}$ are as Equation (2). The higher the reservoir permeability heterogeneity, the greater the β; for

the homogenous reservoir, β = 0. In this study, we researched, under the three conditions of α = 2, α = 5 and α = 10 and under the four conditions of β = 0 (for homogenous reservoir), β = 0.3, β = 0.5 and β = 0.8, the influence of the permeability heterogeneity on the system electricity generation performance. In order to compare the performance of the heterogeneous reservoir with the homogenous reservoir, we calculated and analyzed the production performance of homogenous reservoirs of β = 0 under the conditions of α = 2, α = 5 and α = 10, respectively. The reservoir permeability under different cases are listed in Table 1. Due to geologic sedimentation and compaction, the horizontal permeability decreases with increasing depth under the same material composition, thus in this study, the horizontal permeability declines with increasing depth, and this more agrees with the actual situation.

$$\beta = \sqrt{\sum_{i=1}^{N} \left(\frac{k_{h,i} - k_{h,m}}{k_{h,m}}\right)^2 \Big/ N} = \sqrt{\sum_{i=1}^{N} \left(\frac{k_{v,i} - k_{v,m}}{k_{v,m}}\right)^2 \Big/ N} \quad (1)$$

$$k_{h,m} = \frac{\sum_{i=1}^{N} k_{h,i}}{N}, k_{v,m} = \frac{\sum_{i=1}^{N} k_{v,i}}{N} \quad (2)$$

Table 1. Permeability distribution in the 12 fractured reservoirs.

Case	α	β	k (10^{-15} m^2)	L1	L2	L3	L4	L5	L6	L7	L8
1	2	0	k_h	50	50	50	50	50	50	50	50
			k_v	25	25	25	25	25	25	25	25
2		0.3	k_h	70	65	63	60	40	37	35	30
			k_v	35	32.5	31.5	30	20	18.5	17.5	15
3		0.5	k_h	80	78	70	68	32	30	22	20
			k_v	40	39	35	34	16	15	11	10
4		0.8	k_h	95	90	88	85	15	12	10	5
			k_v	47.5	45	44	42.5	7.5	6	5	2.5
5	5	0	k_h	50	50	50	50	50	50	50	50
			k_v	10	10	10	10	10	10	10	10
6		0.3	k_h	70	65	63	60	40	37	35	30
			k_v	14	13	12.6	12	8	7.4	7	6
7		0.5	k_h	80	78	70	68	32	30	22	20
			k_v	16	15.6	14	13.6	6.4	6	4.4	4
8		0.8	k_h	95	90	88	85	15	12	10	5
			k_v	19	18	17.6	17	3	2.4	2	1
9	10	0	k_h	50	50	50	50	50	50	50	50
			k_v	5	5	5	5	5	5	5	5
10		0.3	k_h	70	65	63	60	40	37	35	30
			k_v	7	6.5	6.3	6	4	3.7	3.5	3
11		0.5	k_h	80	78	70	68	32	30	22	20
			k_v	8	7.8	7	6.8	3.2	3.0	2.2	2.0
12		0.8	k_h	95	90	88	85	15	12	10	5
			k_v	9.5	9	8.8	8.5	1.5	1.2	1	0.5

L1 stands for the topmost layer and L8 stands for the bottommost layer.

2.2. Domain, Grid and Parameters

In order to investigate the influence of vertical permeability heterogeneity on the heat production performance of EGS reservoirs, we first researched the production performance of a homogenous EGS reservoir, then we compared the production performance of the heterogeneous reservoirs with that of the homogenous reservoirs. Figure 2 shows the grid system used in this simulation. There are 25 gridblocks in the x direction and in the y direction, and every length of the gridblocks is 20 m. In the z direction, there are 8 gridblocks, and every height of the gridblocks is 50 m. Thus, the three-dimensional grid system in Figure 2 comprises a total of 25 × 25 × 8 = 5000 gridblocks. A mesh independence check was done to make sure the computation results were not influenced by the mesh division. Table 2 shows the properties and conditions of the simulated domain of the 950–1350 m fractured reservoir [2,6]. According to previous studies, the bottomhole injection pressure P_{inj} must be lower than an upper limit P_{max} [2,6]:

$$P_{inj} < P_{max} \quad (3)$$

where $P_{max} = P_{W0} + P_b$ [2,6]; P_{W0} is the initial pressure of the wellbore and P_b is the maximum pressure buildup. In this study, the perforated interval of the injection well is located at −1350−−1300 m and the perforated interval of the production well is located at −1000−−950 m. The intermediate depth of the injection perforated interval is z = −1325 m, corresponding to an initial pressure of P_{W0} = 11.35 MPa. Based on the engineering data at the Desert Peak geothermal field, P_b can be assigned as 6.90 MPa [5]. So P_{max} = (11.35 + 6.90) MPa = 18.25 MPa. The intermediate depth of the production perforated interval is z = −975 m, corresponding to an initial pressure of 8.23 MPa. According to the engineering data at the Desert Peak geothermal field, the maximum pressure drawdown is 3.40 MPa, thus the minimum pressure at the bottomhole of the production well is about (8.23 − 3.40) MPa = 4.83 MPa. In this study, we assume that the production well is kept at P_0 = 5.0 MPa to maintain the heat production. Based on (3), the maximum water production rate can be determined. The injection temperature is T_{inj} = 60 °C [4,5]; for an initial wellbore pressure of P_{W0} = 11.35 MPa, the injection specific enthalpy is about h_{inj} = 260.66 kJ/kg.

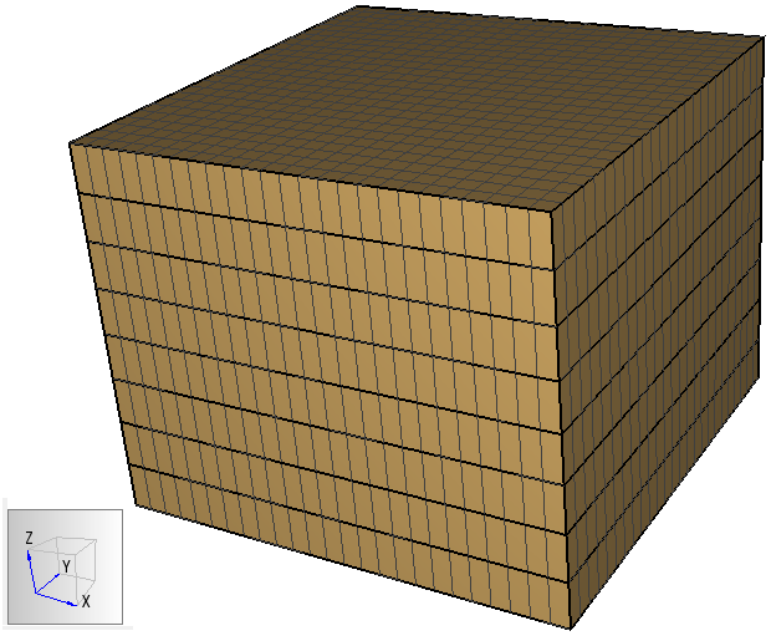

Figure 2. Grid used for domain discretization and numerical computation.

Table 2. The 950–1350 m reservoir properties and conditions at well ZK4001 [2,6].

Parameter	Value
Rock thermal conductivity	2.50 W/(m·K)
Rock specific heat	1000 J/(kg·K)
Rock density	2650 kg/m^3
Reservoir height	400 m
Reservoir length (simulated domain)	500 m
Reservoir width (simulated domain)	500 m
Reservoir porosity	10%
Reservoir horizontal permeability k_h (case1)	50×10^{-15} m^2
Reservoir vertical permeability k_v (case1)	25×10^{-15} m^2
Bottomhole production pressure P_0	5.00 MPa
Productivity index PI	5.0×10^{-12} m^3
Injection temperature	60 °C (260.66 kJ/kg)
Initial temperature	248 °C
Initial pressure	$P = -0.0089z - 0.4444$ (MPa)

2.3. Boundary and Initial Conditions

The saturated vapor pressure corresponding to 248 °C is 3.84 MPa, far lower than the bottomhole pressure at the production well of 5.00 MPa, so the water in the reservoir and wells is all maintained as a liquid. The initial reservoir pressure is $P = -0.0089z - 0.4444$ (MPa), and the initial reservoir temperature is 248 °C [2,6]. Due to symmetry, the lateral boundaries in Figure 2 are no-flow for mass and heat. As stated above, because the slight conductive heat exchange between the permeable reservoir and the impermeable cap rock or base rock is neglected, the boundaries at the top and bottom of the reservoir in Figure 2 are also no-flow for mass and heat. The relative convergence error is assigned as 1.0×10^{-5} and the absolute convergence error is assigned as 1.0 for every conservation equation.

3. Results and Discussion

3.1. Water Production Rate

Table 3 shows the maximum water production rate $Q = 4q$ under the various conditions of permeability distribution shown in Table 1. According to (3), P_{inj} will increase with increasing q, and the maximum q can be obtained only when the P_{inj} is closing to the P_{max}. When the $\alpha = 2$, comparing case 1 with case 2, case 3 and case 4, we can find the water production rate q decreases with the increasing of the degree of reservoir vertical heterogeneity β; under the condition of the homogenous reservoir of $\beta = 0$, the system obtains a maximum water production rate. When the $\alpha = 5$ or $\alpha = 10$, comparing case 5 with case 6, case 7 and case 8, or comparing case 9 with case 10, case 11 and case 12, we can find that only under the condition of the homogenous reservoir of $\beta = 0$, the system obtains a maximum water production rate; with the increasing of the degree of reservoir vertical heterogeneity, the β increases and the water production rate q declines. When the $\beta = 0$, comparing case 1 with case 5 and case 9, we can find that the vertical permeability k_v has an important influence on the water production rate q, and higher vertical permeability will obviously increase the q. Similarly, comparing the group of $\beta = 0.3$, the group of $\beta = 0.5$ or the group of $\beta = 0.8$ in Table 1, we can find similar conclusions. Overall, when the average value of the horizontal permeability of the layered reservoir is constant, the water production rate q will decrease with the increasing of the degree of reservoir vertical heterogeneity β.

Table 3. The water production rate $Q = 4q$ under various conditions of permeability distribution.

Case	1	2	3	4	5	6	7	8	9	10	11	12
q(kg/s)	25.0	20.0	15.0	4.5	23.0	18.0	12.0	3.5	20.0	15.0	11.0	3.0
Q(kg/s)	100.0	80.0	60.0	18.0	92.0	72.0	48.0	14.0	80.0	60.0	44.0	12.0

3.2. Production Temperature

Figure 3 shows the evolution of the production temperature under various conditions of permeability distribution, shown in Table 1, over 50 years of heat production [2,6]. When $\alpha = 2$, comparing case 1 with case 2, case 3 and case 4, we can easily find that with the increasing of the degree of reservoir vertical heterogeneity β, the duration of the stable stage gradually increases, the duration of the declining stage gradually decreases, and the production temperature during the declining stage slowly increases. When $\alpha = 5$ or $\alpha = 10$, comparing case 5 with case 6, case 7 and case 8, or comparing case 9 with case 10, case 11 and case 12, we can obtain similar findings. When $\beta = 0$, comparing case 1 and case 5, case 9, we can find that with the increasing of α, the duration of the stable stage slowly increases, the duration of the declining stage slowly decreases, and the production temperature during the declining stage gradually increases. When the $\beta = 0.3$, $\beta = 0.5$ or $\beta = 0.8$, through comparison we can obtain similar findings. Overall, when the average value of the horizontal permeability of the layered reservoir is constant, with the increasing of the degree of reservoir vertical heterogeneity β, the duration of the declining stage gradually decreases, and the production temperature during the declining stage slowly increases. This is in good agreement with the fact that the q decreases with the increasing of the degree of reservoir vertical heterogeneity β and a lower q obtains a higher production temperature during the declining stage.

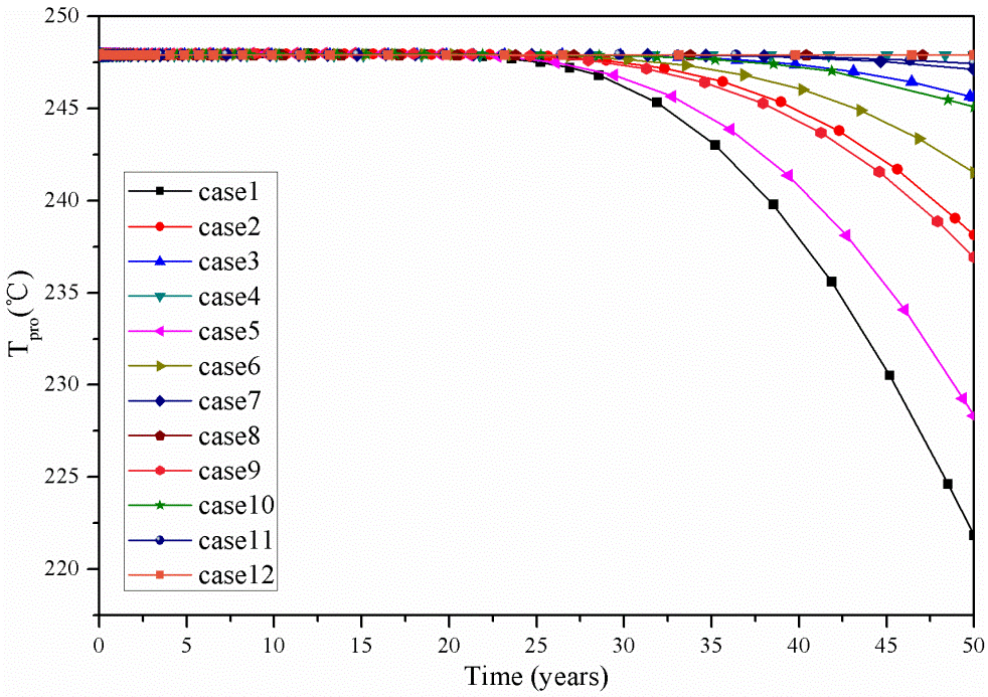

Figure 3. Evolution of production temperature under various conditions of permeability distribution.

3.3. Electric Power

The electric power W_e is calculated as Equation (4) in reference [4], where the injection specific enthalpy h_{inj} is h_{inj} = 260.66 kJ/kg. The Yangbajing geothermal power plant comprises a single-flash power plant and double-flash power plant, which are open loop systems. The heat rejection temperature of the Yangbajing geothermal power plant is T_0 = 9 °C = 282.15 K [2,6].

$$W_e = 0.45Q(h_{pro} - h_{inj})(1 - \frac{T_o}{T_{pro}}) = 1.8q(h_{pro} - h_{inj})(1 - \frac{T_o}{T_{pro}}) \quad (4)$$

Figure 4 shows the evolution of electric power under various conditions of permeability distribution in Table 1 over 50 years of heat production. When $\alpha = 2$, comparing case 1 with case 2, case 3 and case 4, we can easily find that with the increasing of the degree of reservoir vertical heterogeneity β, the electric power gradually decreases. Higher β obviously decreases the q, which prolongs the duration of the stable stage, decreases the duration of the declining stage, and, meanwhile, obviously declines the electric power over the declining stage. When $\alpha = 5$ or $\alpha = 10$, we can obtain similar findings through comparisons. When $\beta = 0$, comparing case 1 with case 5, case 9, we can find that with the increasing of α, the duration of the stable stage gradually increases, and the electric power during the stable stage also gradually decreases; the duration of the declining stage slowly decreases, and the electric power over the declining stage also slowly declines. When $\beta = 0.3$, or $\beta = 0.5$ or $\beta = 0.8$, we can obtain similar findings through comparisons. This is mainly because the reservoir vertical heterogeneity obviously influences the water production rate, and according to Equation (4), this will significantly affect the electric power. Overall, when the average value of the horizontal permeability of the layered reservoir is constant, for a homogenous reservoir, the system will obtain maximum electric power; with the increasing of the reservoir vertical heterogeneity, the electric power will gradually decline.

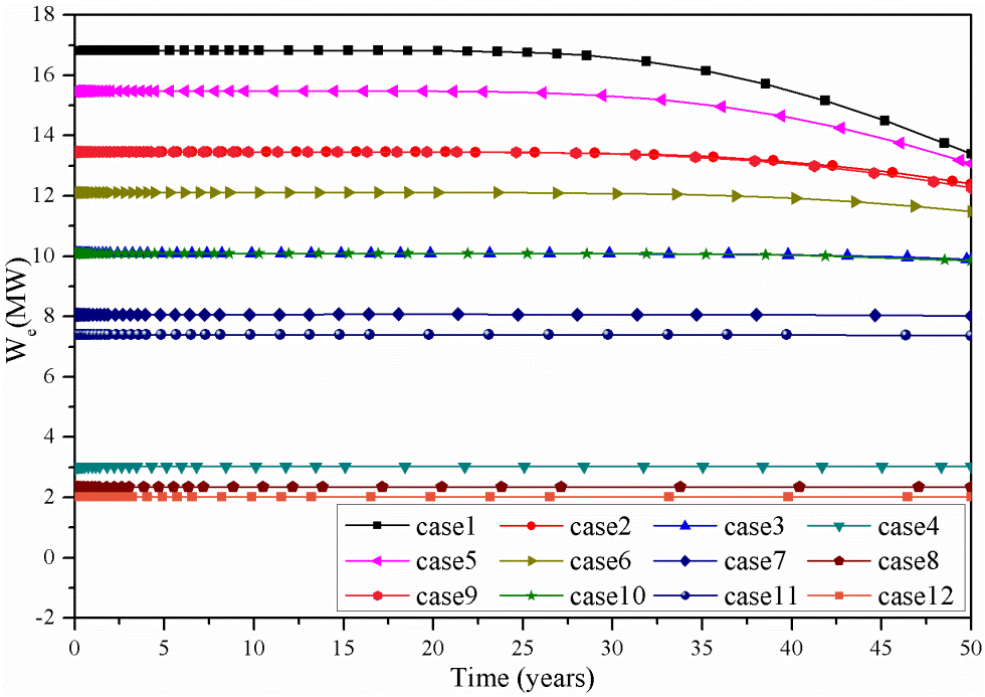

Figure 4. Evolution of electric power under various conditions of permeability distribution.

3.4. Injection Pressure

Figure 5 shows the evolution of the injection pressure under the various conditions of permeability distribution, shown in Table 1, over 50 years of heat production. When $\alpha = 2$, for $\beta = 0$, $\beta = 0.3$, $\beta = 0.5$ and $\beta = 0.8$, the injection pressure is 11.85–17.11 MPa, 11.85–17.92 MPa, 11.78–18.30 MPa and 11.53–18.43 MPa, respectively. So, with the increasing of the reservoir vertical heterogeneity β, the P_{inj} has only a very slight change. When $\alpha = 5$ or $\alpha = 10$, through comparisons, we can easily obtain similar findings. When $\beta = 0$, for $\alpha = 2$ (case 1), $\alpha = 5$ (case 5) and $\alpha = 10$ (case 9), the corresponding P_{inj} is 11.85–17.11 MPa, 11.82–17.90 MPa and 11.76–17.78 MPa, respectively. So, with the increasing of α, the P_{inj} has also a very slight change. For $\beta = 0.3$, $\beta = 0.5$ and $\beta = 0.8$, through comparisons, we can easily obtain similar findings. Overall, the reservoir vertical heterogeneity β has only a very slight influence on the P_{inj} and it is not the main factor affecting the injection pressure. Figure 6 also displays the P_{inj} slowly

increasing during heat production (see Section 3.5). This is because the reservoir impedance is gradually increasing; when the production pressure is constant, based on Equation (5), the P_{inj} will gradually increase.

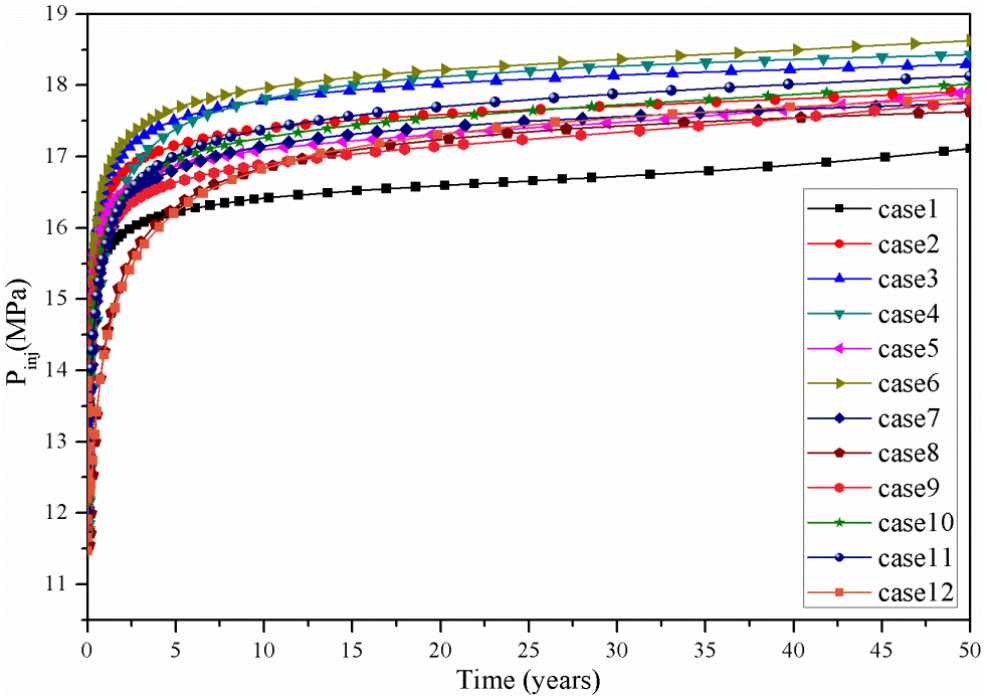

Figure 5. Evolution of injection pressure under various conditions of permeability distribution.

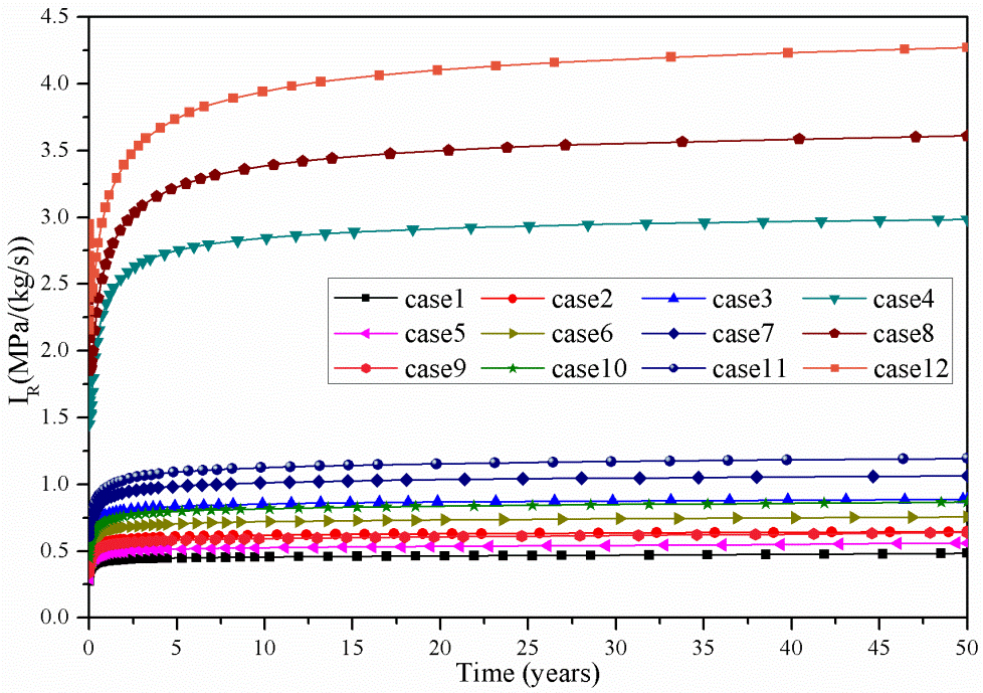

Figure 6. Evolution of reservoir impedance under various conditions of permeability distribution.

3.5. Reservoir Impedance

The reservoir impedance I_R is calculated as Equation (5) [4,5]:

$$I_R = (P_{inj} - P_{pro})/q \quad (5)$$

where I_R represents the power consumption of the unit production rate for penetrating the fractured reservoir, the $P_{pro} = P_0 = 5.00$ MPa is the bottomhole production pressure, and q is the water production rate between the injection well and the production well. Figure 6 displays the evolution of the reservoir impedance under various conditions of permeability distribution, shown in Table 1, over 50 years of heat production. When $\alpha = 2$, for $\beta = 0$, $\beta = 0.3$, $\beta = 0.5$ and $\beta = 0.8$, the corresponding I_R is 0.27–0.48 MPa/(kg/s), 0.34–0.65 MPa/(kg/s), 0.45–0.89 MPa/(kg/s) and 1.45–2.98 MPa/(kg/s), respectively. It can be found that with the increasing of reservoir vertical heterogeneity β, the I_R gradually increases. For $\alpha = 5$ or $\alpha = 10$, through comparisons, we can easily obtain similar findings. When $\beta = 0$, for $\alpha = 2$, $\alpha = 5$ and $\alpha = 10$, the I_R is 0.27–0.48 MPa/(kg/s), 0.30–0.56 MPa/(kg/s) and 0.34–0.64 MPa/(kg/s), respectively. So, with the increasing of α, the system I_R gradually increases. For $\beta = 0.3$, $\beta = 0.5$ and $\beta = 0.8$, through comparisons, we can easily get similar findings. As stated in Section 3.1, this is because a higher reservoir heterogeneity obviously decreases the water production rate. When the P_{inj} basically maintains at a constant, according to Equation (5), this will obviously increase the I_R. Overall, when the average value of the horizontal permeability of the layered reservoir is constant, for the homogenous reservoir, the system will obtain a minimum I_R; with the increasing of reservoir vertical heterogeneity β, the I_R gradually increases. This proves that the stimulation of an EGS reservoir should be controlled as homogeneously as possible to obviously reduce the I_R. Figure 6 also shows that during heat production, the I_R gradually increases. This is because with the heat production, the temperature of the reservoir rock and fluid gradually declines, causing the slow increase in water viscosity, and this finally causes increasing of the I_R. This has been reported in detail in previous studies from Zeng et al. [2,4,6].

3.6. Pump Power

The internal energy consumption W_p of both the injection pump and production pump can be calculated as Equation (6) [4]:

$$W_p = \frac{4q(P_{inj} - P_{pro}) - 4q\rho g(h_1 - h_2)}{\rho \eta_p} \quad (6)$$

where h_1 is the depth of the injection well and h_2 is the depth of the production well. In this work, $h_1 = 1325.0$ m, $h_2 = 975.0$ m and $h_1 - h_2 = 350.0$ m. The water density ρ changes versus the temperature and pressure, and this will obviously influence the calculation of W_p [4,5]. In this study, the average values of the maximum density and the minimum density are adopted for calculations in Equations (6) and (7), and this treatment method has proved to be effective in previous studies [4,5]. The maximum density is 998.0 kg/m^3 and the minimum density is 804.0 kg/m^3, thus the average value of $\rho = 901.0$ kg/m^3 is adopted for calculations in Equations (6) and (7). Figure 7 displays the evolution of the pump power under the various conditions of permeability distribution in Table 1 over 50 years of heat production. When $\alpha = 2$, for $\beta = 0$, $\beta = 0.3$, $\beta = 0.5$ and $\beta = 0.8$, the corresponding W_p is 0.52–1.25 MW, 0.42–1.09 MW, 0.31–0.85 MW and 0.09–0.26 MW, respectively. It can be found that for the homogenous reservoir ($\beta = 0$), the system obtains maximum W_p; with the increasing of reservoir vertical heterogeneity β, the W_p gradually declines. This is mainly because with the increasing of reservoir vertical heterogeneity β, the q gradually decreases, according to Equation (6), and the W_p gradually declines. For $\alpha = 5$ or $\alpha = 10$, we can get similar findings through comparisons. When $\beta = 0$, for $\alpha = 2$, $\alpha = 5$ and $\alpha = 10$, the corresponding W_p is 0.52–1.25 MW, 0.48–1.25 MW and 0.41–1.08 MW, respectively. So, with the increasing of α, the q gradually declines and the W_p gradually decreases. For $\beta = 0.3$, $\beta = 0.5$ and $\beta = 0.8$, we can obtain similar findings through comparisons.

Overall, the reservoir vertical heterogeneity has a significant influence on the W_p when the average value of the horizontal permeability of the layered reservoir is constant and the W_p gradually declines with the increasing of the reservoir vertical heterogeneity; for a homogenous reservoir, the system obtains a maximum W_p. Figure 7 also shows that the W_p gradually increases with heat production, and this is because the P_{inj} gradually increases with time; these are in good agreement with previous studies from Zeng et al. [2,4–6].

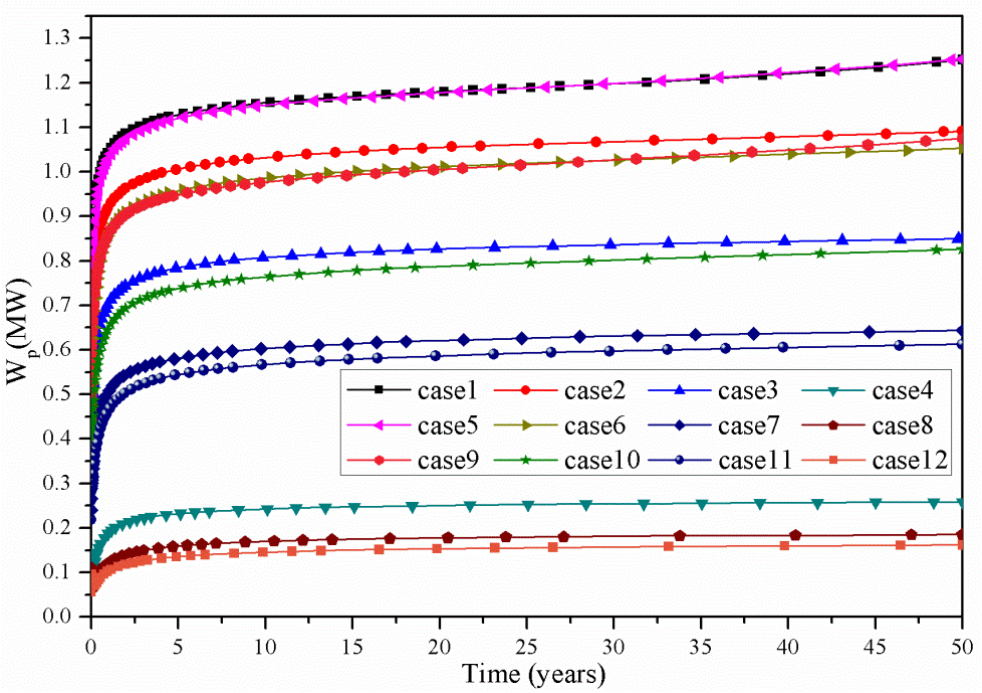

Figure 7. Evolution of pump power under various conditions of permeability distribution.

3.7. Energy Efficiency

The energy efficiency η of the system can be calculated as Equation (7) based on [4,5]:

$$\eta = \frac{W_e}{W_p} = \frac{0.45\rho\eta_p(h_{pro} - h_{inj})(1 - T_o/T_{pro})}{(P_{inj} - P_{pro}) - \rho g(h_1 - h_2)} \quad (7)$$

As stated above, the average value of the water density of ρ = 901.0 kg/m^3 is adopted in the calculation of Equation (7). Figure 8 displays the evolution of the energy efficiency under the various conditions of permeability distribution in Table 1 over 50 years of heat production. When α = 2, for β = 0, β = 0.3, β = 0.5 and β = 0.8, the corresponding η is 32.29–10.70, 32.27–11.36, 32.83–11.65 and 35.27–11.72, respectively. It can be found that the reservoir vertical heterogeneity β has only a very slight influence on the η. When α = 5 or α = 10, we can get similar findings through comparisons. When β = 0, for α = 2, α = 5 and α = 10, the corresponding η is 32.29–10.70, 32.53–10.44 and 33.04–11.41, respectively; it can be found that the α also has only a very slight influence on the η. When β = 0.3, β = 0.5 or β = 0.8, we can get similar findings through comparisons. Overall, when the average value of the horizontal permeability of the layered reservoir is constant, the reservoir vertical heterogeneity has only a very slight influence on the η. According to Equation (7), this is because the reservoir vertical heterogeneity has only a very slight influence on the P_{inj} as stated in Section 3.4; meanwhile, it has also a very slight influence on the h_{pro}, thus the reservoir vertical heterogeneity has only very slight influence on the η. Figure 8 also shows that the η will decline during the heat production. This is because the P_{inj} will gradually increase and h_{pro} and T_{pro} will gradually decline; this is in good accordance with previous studies from Zeng et al. [2,4,5].

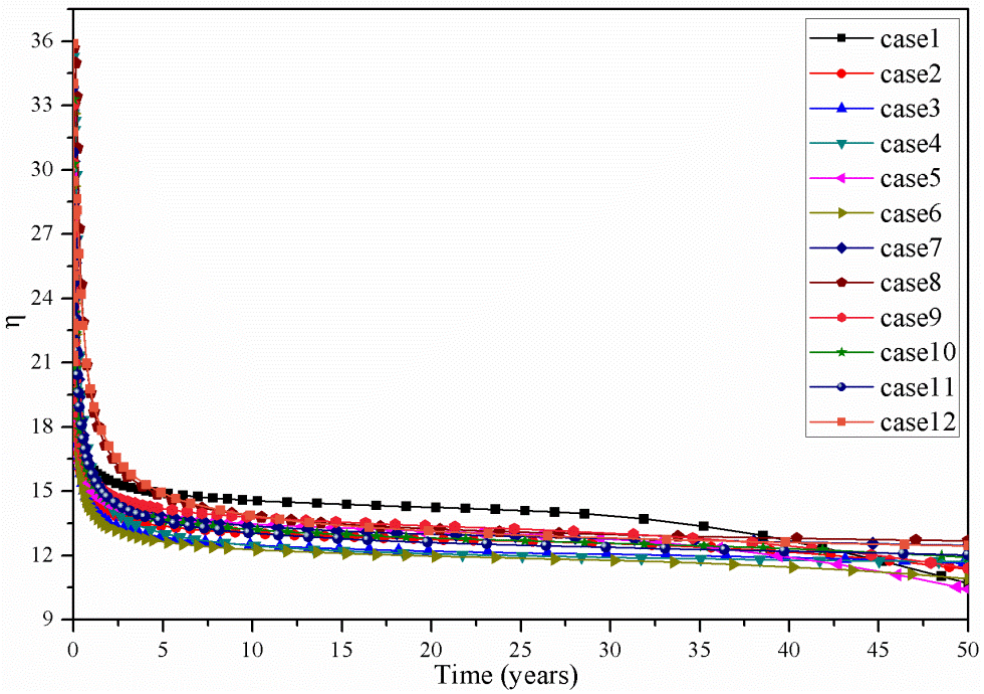

Figure 8. Evolution of energy efficiency under various conditions of permeability distribution.

4. Model Validation

Strictly, the numerical results should be compared with the experimental data to make sure that the computation is accurate and reliable. However, because the experimental modeling of geothermal production is complex and time-consuming, until now, experimental data about heat production at the Yangbajing geothermal field have been scarce. For simplification, we compared the results of Case 1 in this work with a previous study in reference [8], where most of the model conditions and properties are basically the same. Figure 9 shows the comparison of the production temperatures between Case 1 in this work and the basic case in [8]. In Case 1, the production temperature drops from 248.0 °C to 221.8 °C over 50 years, while in the basic case in [8], the production temperature drops from 248.0 °C to 232.5 °C over 50 years. The relative error of the production temperature between the two cases increases with time, and finally, it reaches 4.8%, which is much smaller than 10%. Because the results of the two simulated cases are very close (relative error is smaller than 5%), we can regard the simulations in this work as reliable.

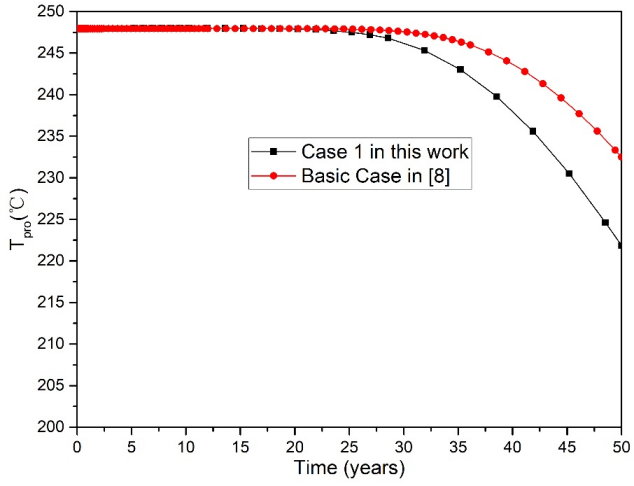

Figure 9. Comparison of production temperatures in Case 1 in this work and basic case in [8].

5. Conclusions

In this work, we numerically investigated the effect of vertical permeability heterogeneity on the electricity generation performance of EGS based on the geological data at the Yangbajing geothermal field. Based on the study, the following conclusions are made.

(1) When the average value of the horizontal permeability of the layered reservoir is constant, for a homogenous reservoir, the system obtains a maximum water production rate.
(2) When the average value of the horizontal permeability of the layered reservoir is constant, with the increasing of the reservoir permeability heterogeneity, the duration of the declining stage gradually declines and the production temperature during the declining stage gradually increases.
(3) When the average value of the horizontal permeability of the layered reservoir is constant, for a homogenous reservoir, the system obtains a maximum electric power.
(4) When the average value of the horizontal permeability of the layered reservoir is constant, for a homogenous reservoir, the system obtains a minimum reservoir impedance.
(5) When the average value of the horizontal permeability of the layered reservoir is constant, for a homogenous reservoir, the system obtains a maximum pump power.
(6) When the average value of the horizontal permeability of the layered reservoir is constant, with the increasing of the vertical permeability heterogeneity, the water production rate gradually decreases, the electric power gradually declines, the reservoir impedance gradually increases, and the pump power gradually declines.
(7) When the average value of the horizontal permeability of the layered reservoir is constant, with the increasing of the reservoir permeability heterogeneity, the injection pressure and energy efficiency have only very slight changes. This proves that the reservoir permeability heterogeneity is not the main factor affecting the injection pressure and energy efficiency.

Author Contributions: Formal analysis: Y.Z.; Methodology: Y.Z., F.S.; Writing: Y.Z.; Review: H.Z. All authors have read and agreed to the published version of the manuscript.

Funding: The study was financially supported by the GDAS' Project of Science and Technology Development (2020GDASYL-20200102020, 2020GDASYL-20200102013, 2020GDASYL-20200301003, 2020GDASYL-20200402003, 2020GDASYL-20200302007, 2019GDASYL-0102002), Guangdong Foundation for Program of Science and Technology Research (2019B121205006, 2019B121201004), the National Natural Science Foundation of China (NSFC: 41930865) and Open Foundation of Key Laboratory of Natural Gas Hydrate, CAS(E0290206). We also thank the Northern Guangdong Soil Environment Observation and Research Station, and the Guangdong Engineering Center of Non-point Source Pollution Control for their support.

Data Availability Statement: The software tool TOUGH2 are available for download. The most recent versions are available for download from https://www.thunderheadeng.com/petrasim/ accessed on 2 April 2021.

Acknowledgments: The authors are grateful for the comments by Nengyou Wu at the Qingdao Institute of Marine Geology, China Geological Survey, which significantly improved the manuscript.

Conflicts of Interest: The authors declare that there is no conflict of interest.

Nomenclature

g	gravity, 9.80 m/s^2
h	well depth, m
h_1	depth of injection well, m
h_2	depth of production well, m
h_{inj}	injection specific enthalpy, kJ/kg
h_{pro}	production specific enthalpy, kJ/kg
I_R	reservoir impedance, MPa/(kg/s)

k	reservoir permeability, m^2
k_f	fracture permeability, m^2
k_m	matrix permeability, m^2
k_x	intrinsic permeability along x, m^2
k_y	intrinsic permeability along y, m^2
k_z	intrinsic permeability along z, m^2
P	pressure, MPa
P_{max}	critical pressure, MPa
P_{inj}	injection pressure, MPa
P_{pro}	production pressure, MPa
P_0	bottomhole production pressure, MPa
q	water production rate, kg/s
Q	total water production rate, kg/s
T	temperature, °C
T_0	mean heat rejection temperature, 282.15 K
T_{pro}	production temperature, °C
W_p	electric power of pump, MW
W_e	electric power, MW
x, y, z	cartesian coordinates, m
ϕ	reservoir porosity
η	energy efficiency
η_p	pump efficiency, 80%
ρ	water density, kg/m^3

References

1. Tester, J.W.; Livesay, B.; Anderson, B.J.; Moore, M.C.; Bathchelor, A.S.; Nichols, K.; Blackwell, D.D.; Petty, S.; DiPippo, R.; Toksöz, M.N.; et al. *The Future of Geothermal Energy: Impact of Enhanced Geothermal Systems (EGS) on the United States in the 21st Century*; An assessment by an MIT-led interdisciplinary panel; Massachusetts Institute of Technology: Cambridge, MA, USA, 2006.
2. Zeng, Y.; Zhan, J.; Wu, N.; Luo, Y.; Cai, W. Numerical investigation of electricity generation potential from fractured granite reservoir by water circulating through three horizontal wells at Yangbajing geothermal field. *Appl. Therm. Eng.* **2016**, *104*, 1–15. [CrossRef]
3. Wang, J.; Hu, S.; Pang, Z.; He, L.; Zhao, P.; Zhu, C.; Rao, S.; Tang, X.; Kong, Y.; Luo, L.; et al. Estimate of geothermal resources potential for hot dry rock in the continental area of China. *Sci. Technol. Rev.* **2012**, *30*, 25–31. (In Chinese)
4. Zeng, Y.C.; Su, Z.; Wu, N.Y. Numerical simulation of heat production potential from hot dry rock by water circulating through two horizontal wells at Desert Peak geothermal field. *Energy* **2013**, *56*, 92–107. [CrossRef]
5. Zeng, Y.C.; Wu, N.Y.; Su, Z.; Wang, X.X.; Hu, J. Numerical simulation of heat production potential from hot dry rock by water circulating through a novel single vertical fracture at Desert Peak geothermal field. *Energy* **2013**, *63*, 268–282. [CrossRef]
6. Zeng, Y.C.; Wu, N.Y.; Su, Z.; Hu, J. Numerical simulation of electricity generation potential from fractured granite reservoir through a single horizontal well at Yangbajing geothermal field. *Energy* **2014**, *65*, 472–487. [CrossRef]
7. Zeng, Y.C.; Zhan, J.M.; Wu, N.Y.; Luo, Y.Y.; Cai, W.H. Numerical investigation of electricity generation potential from fractured granite reservoir through a single vertical well at Yangbajing geothermal field. *Energy* **2016**, *114*, 24–39. [CrossRef]
8. Zeng, Y.C.; Zhan, J.M.; Wu, N.Y.; Luo, Y.Y.; Cai, W.H. Numerical simulation of electricity generation potential from fractured granite reservoir through vertical wells at Yangbajing geothermal field. *Energy* **2016**, *103*, 290–304. [CrossRef]
9. Zeng, Y.; Tang, L.; Wu, N.; Cao, Y. Analysis of influencing factors of production performance of enhanced geothermal system: A case study at Yangbajing geothermal field. *Energy* **2017**, *127*, 218–235. [CrossRef]
10. Zhang, Y.J.; Li, Z.W.; Guo, L.L.; Gao, P.; Jin, X.P.; Xu, T.F. Electricity generation from enhanced geothermal systems by oilfield produced water circulating through reservoir stimulated by staged fracturing technology for horizontal wells: A case study in Xujiaweizi area in Daqing Oilfield, China. *Energy* **2014**, *78*, 788–805. [CrossRef]
11. Zhang, Y.J.; Guo, L.L.; Li, Z.W.; Yu, Z.W.; Xu, T.F.; Lan, C.Y. Electricity generation and heating potential from enhanced geothermal system in Songliao Basin, China: Different reservoir stimulation strategies for tight rock and naturally fractured formations. *Energy* **2015**, *93*, 1860–1885. [CrossRef]
12. Zhang, Y.J.; Li, Z.W.; Yu, Z.W.; Guo, L.L.; Jin, X.P.; Xu, T.F. Evaluation of developing an enhanced geothermal heating system in northeast China: Field hydraulic stimulation and heat production forecast. *Energy Build.* **2015**, *88*, 1–14. [CrossRef]
13. Huang, X.X.; Zhu, J.L.; Niu, C.G.; Li, J.; Hu, X.; Jin, X. Heat extraction and power production forecast of a prospective Enhanced Geothermal System site in Songliao Basin, China. *Energy* **2014**, *75*, 360–370. [CrossRef]
14. Huang, X.X.; Zhu, J.L.; Li, J.; Lan, C.Y.; Jin, X.P. Parametric study of an enhanced geothermal system based on thermo-hydro-mechanical modeling of a prospective site in Songliao Basin. *Appl. Therm. Eng.* **2016**, *105*, 1–7. [CrossRef]

15. Feng, Y.; Chen, X.; Xu, X.F. Current status and potential of enhanced geothermal system in China: A review. *Renew. Sustain. Energy Rev.* **2014**, *33*, 214–223. [CrossRef]
16. Franco, A.; Vaccaro, M. Numerical simulation of geothermal reservoirs for the sustainable design of energy plants: A review. *Renew. Sustain. Energy Rev.* **2014**, *30*, 987–1002. [CrossRef]
17. Zhu, J.L.; Hu, K.Y.; Lu, X.L.; Huang, X.X.; Liu, K.T.; Wu, X.J. A review of geothermal energy resources, development, and application in China: Current status and prospects. *Energy* **2015**, *93*, 466–483. [CrossRef]
18. Pandey, S.N.; Vishal, V.; Chaudhuri, A. Geothermal reservoir modeling in a coupled thermos-hydro-mechanical-chemical approach: A review. *Earth Sci. Rev.* **2018**, *185*, 1157–1169. [CrossRef]
19. Sanyal, S.K.; Butler, S.J. An analysis of power generation prospects from enhanced geothermal systems. In Proceedings of the World Geothermal Congress 2005, Antalya, Turkey, 24–29 April 2005; pp. 1–6.
20. Taron, J.; Elsworth, D.; Min, K. Numerical simulation of thermal-hydrologic-mechanical-chemical processes in deformable, fractured porous media. *Int. J. Rock Mech. Min. Sci.* **2009**, *46*, 842–854. [CrossRef]
21. Taron, J.; Elsworth, D. Thermal-hydrologic-mechanical-chemical processes in the evolution of engineered geothermal reservoirs. *Int. J. Rock Mech. Min. Sci.* **2009**, *46*, 855–864. [CrossRef]
22. Gelet, R.; Loret, B.; Khalili, N. A thermo-hydro-mechanical coupled model in local thermal non-equilibrum for fractured HDR reservoir with double porosity. *J. Geophys. Res.* **2012**, *117*, 1–23.
23. Gelet, R.; Loret, B.; Khalili, N. Thermal recovery from a fractured medium in local thermal non-equilibrium. *Int. J. Numer. Anal. Methods Geomech.* **2013**, *37*, 2471–2501. [CrossRef]
24. Pruess, K. Enhanced geothermal system (EGS) using CO_2 as working fluid-A novel approach for generating renewable energy with simultaneous sequestration of carbon. *Geothermics* **2006**, *35*, 351–367. [CrossRef]
25. Pruess, K. On production behavior of enhanced geothermal systems with CO_2 as working fluid. *Energy Convers. Manag.* **2008**, *49*, 1446–1454. [CrossRef]
26. Zeng, Y.C.; Tang, L.S.; Wu, N.Y.; Cao, Y.F. Numerical simulation of electricity generation potential from fractured granite reservoir using the MINC method at the Yangbajing geothermal field. *Geothermics* **2018**, *75*, 122–136. [CrossRef]
27. Salimzadeh, S.; Nick, H.M. A coupled model for reactive flow through deformable fractures in Enhanced Geothermal Systems. *Geothermics* **2019**, *81*, 88–100. [CrossRef]
28. Shi, Y.; Song, X.Z.; Li, J.C.; Wang, G.S.; Zheng, R.; Yulong, F.X. Numerical investigation on heat extraction performance of a multilateral-well enhanced geothermal system with a discrete fracture network. *Fuel* **2019**, *244*, 207–226. [CrossRef]
29. Wang, Y.; Li, T.; Chen, Y.; Ma, G.W. A three-dimensional thermo-hydro-mechanical coupled model for enhanced geothermal systems (EGS) embedded with discrete fracture networks. *Comput. Methods Appl. Mech. Eng.* **2019**, *356*, 465–489. [CrossRef]
30. Sun, Z.X.; Zhang, X.; Xu, Y.; Yao, J.; Wang, H.X.; Lv, S.H.; Sun, Z.L.; Huang, Y.; Cai, M.Y.; Huang, X. Numerical simulation of the heat extraction in EGS with thermal-hydraulic-mechanical coupling method based on discrete fractures. *Energy* **2017**, *120*, 20–33. [CrossRef]
31. Yao, J.; Zhang, X.; Sun, Z.X.; Huang, Z.Q.; Liu, J.R.; Li, Y.; Xin, Y.; Yan, X.; Liu, W. Numerical simulation of the heat extraction in 3D-EGS with thermal-hydraulic-mechanical coupling method based on discrete fractures model. *Geothermics* **2018**, *74*, 19–34. [CrossRef]
32. Zinsalo, J.M.; Lamarche, L.; Raymond, J. Sustainable electricity generation from an Enhanced geothermal system considering reservoir heterogeneity and water losses with a discrete fractures model. *Appl. Therm. Eng.* **2021**, *192*, 116886. [CrossRef]
33. Jiang, F.M.; Luo, L.; Chen, J.L. A novel three-dimensional transient model for subsurface heat exchange in enhanced geothermal systems. *Int. Commun. Heat Mass Transf.* **2013**, *41*, 57–62. [CrossRef]
34. Jiang, F.M.; Chen, J.L.; Huang, W.B.; Luo, L. A three-dimensional transient model for EGS subsurface thermo-hydraulic process. *Energy* **2014**, *72*, 300–310. [CrossRef]
35. Shaik, A.R.; Rahman, S.S.; Tran, N.H.; Tran, T. Numerical simulation of fluid-rock coupling heat transfer in naturally fractured geothermal system. *Appl. Therm. Eng.* **2011**, *31*, 1600–1606. [CrossRef]
36. Fan, X. *Conceptual Model and Assessment of the Yangbajing Geothermal Field, Tibet, China*; Geothermal Training Programme: Reykjavík, Iceland, 2002.
37. Dor, J.; Zhao, P. Characteristics and genesis of the Yangbajing geothermal field, Tibet. In Proceedings of the World Geothermal Congress 2000, Kyushu-Tohoku, Japan, 28 May–10 June 2000; pp. 1083–1088.
38. Pruess, K.; Oldenburg, C.; Moridis, G. *TOUGH2 User's Guide, Version 2.0*; Lawrence Berkeley National Laboratory: Berkeley, CA, USA, 1999.
39. Luo, F.; Xu, R.N.; Jiang, P.X. Numerical investigation of the influence of vertical permeability heterogeneity in stratified formation and of injection/production well perforation placement on CO_2 geological storage with enhanced CH_4 recovery. *Appl. Energy* **2013**, *102*, 1314–1323. [CrossRef]